

# Micro/Nanoscale Parallel Patterning of Functional Biomolecules, Organic Fluorophores and Colloidal Nanocrystals

S. Sabella · V. Brunetti · G. Vecchio · A. Della Torre ·  
R. Rinaldi · R. Cingolani · P. P. Pompa

Received: 8 May 2009 / Accepted: 1 July 2009 / Published online: 14 July 2009  
© to the authors 2009

**Abstract** We describe the design and optimization of a reliable strategy that combines self-assembly and lithographic techniques, leading to very precise micro-/nanopositioning of biomolecules for the realization of micro- and nanoarrays of functional DNA and antibodies. Moreover, based on the covalent immobilization of stable and versatile SAMs of programmable chemical reactivity, this approach constitutes a general platform for the parallel site-specific deposition of a wide range of molecules such as organic fluorophores and water-soluble colloidal nanocrystals.

**Keywords** Molecular self-assembly · Lithographic techniques · DNA · Green fluorescent proteins · Colloidal nanocrystals

## Abbreviations

SAMs Self-assembled monolayers  
MPTS Mercaptopropyltriethoxysilane  
APTES Aminopropyltriethoxysilane  
NCs Colloidal nanocrystals  
FM Fluorescein-5-maleimide  
SiO<sub>2</sub> Silicon dioxide

PMMA Polymethylmethacrylate  
GFP Green fluorescent protein  
GTA Glutaraldehyde

## Introduction

Considerable efforts have recently been devoted by the nanoscience community to develop reliable patterning methodologies for the spatially controlled deposition of a wide range of molecules, exploiting their spontaneous organization in the form of 2D or 3D matrices onto substrates of different materials (semiconductors, metals, plastics) [1]. Notably, in the case of biological species (such as DNA, proteins, antibodies, cells), the creation of patterned active substrates, enabling precise positioning of biomolecules with nanoscale resolution over large areas, may provide new attractive diagnostic tools to perform more efficient analyses in high throughput [2]. The peculiar self-assembling capabilities of biomolecules may lead to the development of novel bio/inorganic or organic/inorganic active interfaces [3], likely preserving biological functionality upon immobilization, and favoring the possibility to characterize biomolecular interaction events at single molecule level [4]. Interestingly, such hybrid active interfaces may conjugate the specificity and reactivity of the biological “soft machines” to particular electronic or optical characteristics of the “hard substrates” (such as smart plastic films enabling recognition of target biomolecules by optical excitation [5]) and can potentially be applied to a variety of research fields, ranging from biosensors and diagnostics [6, 7] to optoelectronics and microfluidics [8, 9].

To date, several nanofabrication techniques, including plasma deposition and electron beam lithography (EBL)

**Electronic supplementary material** The online version of this article (doi:10.1007/s11671-009-9386-7) contains supplementary material, which is available to authorized users.

S. Sabella · R. Cingolani · P. P. Pompa (✉)  
Italian Institute of Technology (IIT), National Nanotechnology Laboratory, Via Barsanti 1, Arnesano, Lecce 73010, Italy  
e-mail: piero.pompa@unile.it

V. Brunetti · G. Vecchio · A. D. Torre · R. Rinaldi  
National Nanotechnology Laboratory of CNR-INFN,  
Scuola Superiore ISUFI, University of Salento,  
Via Arnesano 16, Lecce 73100, Italy

[10–13], micro-contact printing [14, 15], dip-pen nanolithography [16–18], and screen printing [19], have been exploited for the production of micro- and nanostructured biomolecular substrates. In particular, interesting examples of selective surface patterning, based on the use of optical lithography [20] or PECVD [21] coupled to the formation of different silane-based self-assembled monolayers (SAMs), have recently been reported, demonstrating the selective nanopositioning of proteins and colloidal nanocrystals (NCs) or metallic nanoparticles and NCs. However, while each of the above-mentioned techniques has some remarkable advantages, it seems they are rather complementary and often present significant drawbacks usually associated to possible losses of biomolecular functionality, as well as to the precise spatial control and/or uniformity of the nanostructured active substrate to immobilize probe molecules. In this frame, we show here the design and optimization of a reliable strategy to obtain patterned bioactive surfaces by combining EBL technique to molecular self-assembling. We demonstrate the

possibility to obtain precise micro- and nanopositioning of functional biomolecules (such as DNA and proteins), as well as the simultaneous patterning of organic fluorophores and water-soluble colloidal nanocrystals.

The technological scheme in Fig. 1 describes the multistep process that drives probe (bio)molecules (e.g., ssDNA or antibodies) to be immobilized with high spatial control by a covalent site-specific capture with the functionalized substrate. An appropriate resist mask is initially defined by E-beam lithography with nanometer resolution (steps a and b) to guide the self-assembling of specific molecules from bulk solution only into the exposed area of the substrate (step c), resulting in a spatially controlled functionalization of the substrate upon subsequent resist removal (step d). Such patterned surface reactivity consequently acts as a template for the sequential site-specific self-assembling of cross-linking molecules and probe species (steps e and f), which are, therefore, selectively immobilized from bulk solution into specific areas of the substrate with precise spatial control and avoiding any

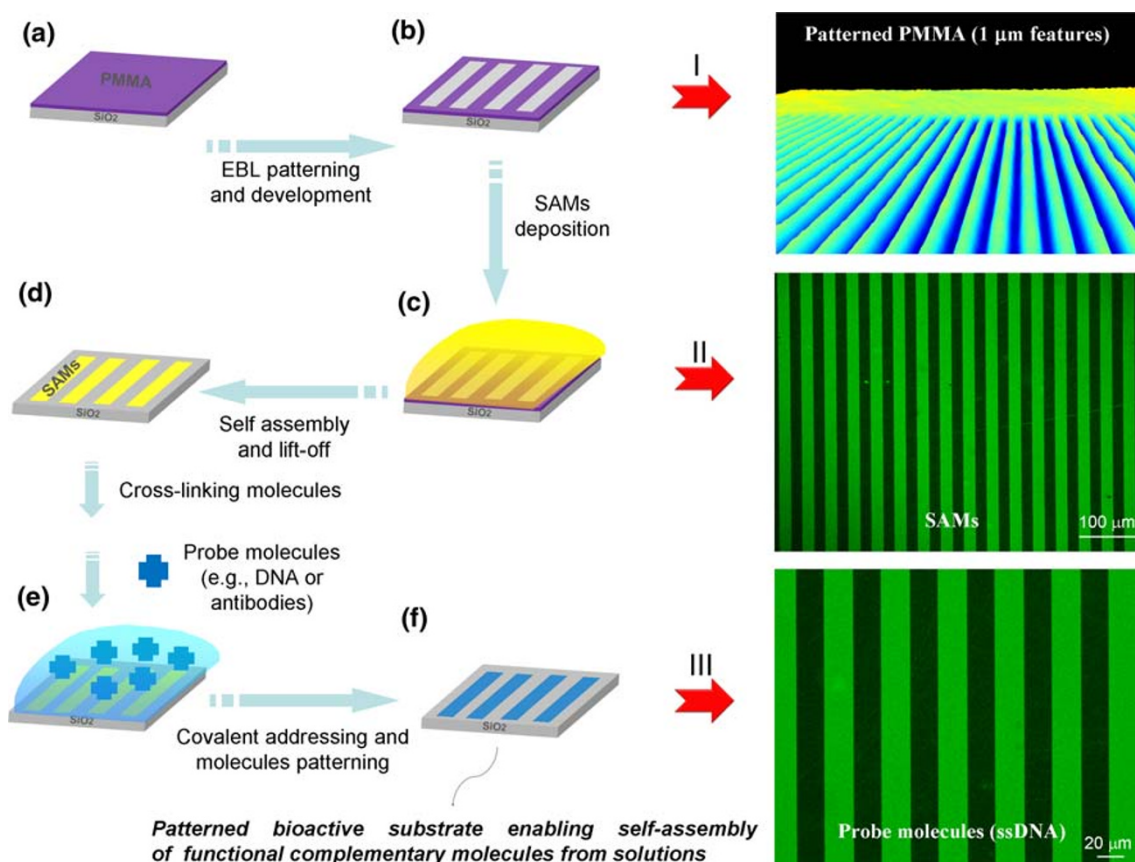


**Fig. 1** Technological scheme for (bio)molecular patterning based on E-beam lithography and multistep self-assembly. *Left:* **a** A resist layer (PMMA) was deposited onto silicon dioxide by spin coating; **b** EBL patterning and development; **c** selective SAM deposition by self-assembly in the exposed regions of the substrate; **d** lift-off; **e**, **f** spatially confined self-assembling of cross-linking molecules and

probe biomolecules. *Right:* real images of the steps **b**, **c** and **f**, respectively. *I* Holographic microscopy 3D image of 1 μm wide PMMA stripes after EBL patterning and development; *II* confocal microscopy image of FITC-labeled APTES stripes (features: 20 μm); and *III* confocal microscopy image of Cy3-labeled ssDNA stripes (features: 20 μm)

significant stress and/or perturbation due to the immobilization process (as possible, for instance, in the case of microcontact printing of biomolecules [22]). This approach may drive the sequential and/or parallel deposition of molecules onto a variety of materials, through site-specific covalent interactions. A wide range of different organic and inorganic molecules may precisely be immobilized by this method, with the unique limitation that compatible chemical reactive groups must properly be selected. In this work, different organic silanes, namely aminopropyltriethoxysilane (APTES) and mercaptopropyltriethoxysilane (MPTS), were tested, and both were found to exhibit remarkable stability and versatility to develop complex self-assembled supramolecular architectures. Importantly, all the conjugation procedures were implemented in physiological reaction environment (aqueous solution, neutral pH), in order to develop a quite general platform to be used for a wide range of applications involving biomolecules such as solid-state biorecognition of target analytes (DNA hybridization, protein/antibody interactions). A representative example of EBL-defined PMMA stripes is reported in Fig. 1(right, I), showing the subsequent guided self-assembling of a patterned SAM of APTES (right, II) followed by the spatially controlled covalent immobilization of ssDNA probe molecules (right, III). The pattern of APTES was inspected by confocal microscopy after conjugation with fluorescein, revealing very precise spatial confinement of the chemical reactivity along with a very good density and uniformity of the molecular SAM in the stripes (see also “Experimental”). The resolution of the patterned SAMs is limited only by EBL, thus allowing the realization of high density

nanoarrays of specific molecules. Patterned APTES were then activated by a homo-bifunctional linker (glutaraldehyde), thus enabling the capturing, from aqueous solution, of amino-terminated biomolecular probes (e.g., ssDNA or antibody). The precise positioning of Cy3-labeled ssDNA into highly homogeneous micrometric stripes is reported in Fig. 1(right, III).

The retention of the biological functionality of such DNA probe molecules, immobilized in the solid state with various spatial resolutions (down to submicron features), was subsequently assessed by probing their specific reactivity toward a solution containing a complementary target sequence (see “Experimental” for details). Hybridization events were displayed by an appropriate fluorescent reporter, i.e., SYBR Green I, an intercalating dye, highly specific for double strand DNA. Figure 2 reveals the high spatial control offered by our combined strategy. Hybridization reactions were precisely localized onto the substrate, even in the case of nanoscale features (500 nm wide stripes or squares), showing a very good uniformity of the immobilized DNA molecules as well as a complete absence of aspecific background signal in the external regions of the designed patterns (see also the fluorescence line profile reported in the inset of Fig. 2a). The reliability of the approach was further confirmed by testing the specificity of the solid-state DNA–DNA interactions using a target sequence with a single mismatch. In this latter case, the same patterns were observed but the fluorescence signals, and thus the hybridization efficiencies, were found to be significantly lower, namely  $\sim 15\text{--}20\%$  of the value observed with the complementary sequence (data not shown). DNA patterns were also characterized by atomic

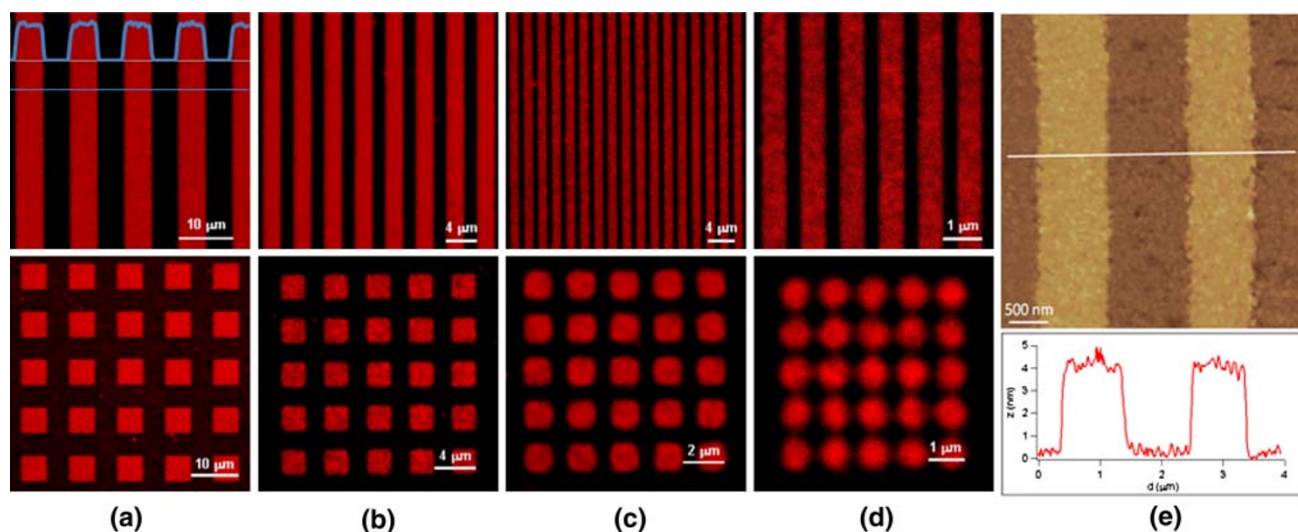


**Fig. 2** Micro- and nanoscale patterning of functional DNA. **a–d** confocal microscopy images of hybridized DNA (dsDNA), with features of 5  $\mu\text{m}$  (**a**) 2  $\mu\text{m}$  (**b**) 1  $\mu\text{m}$  (**c**) and 0.5  $\mu\text{m}$  (**d**); a

fluorescence line profile of the DNA stripes is also reported in the inset of (**a**). **e** Representative atomic force microscopy (AFM) image and AFM line profile of a DNA pattern with 1  $\mu\text{m}$  wide stripes

force microscopy (AFM) (Fig. 2, right), clearly confirming the very precise spatial confinement of the hybridization reaction.

The same multistep strategy (Fig. 1) was also used to demonstrate the production of highly packed micro- and nanoarrays of functional antibodies for protein sensing and patterning. Such immunosensors were realized by exploiting the ability of patterned APTES to address, with nanometer spatial control, the immobilization of more complex and larger biomolecules, such as antibodies, while preserving their functional status. We used Anti-TurboGFP as a model. Antibodies immobilization was optimized in terms of concentration and incubation conditions in order to obtain a good and homogeneous biomolecular coverage, while avoiding aspecific antibodies physisorption onto the substrate (see “Experimental”). The specific reactivity and the maintenance of the biological activity of the antibodies arrays were assessed by performing an immunoassay, namely the optical detection of the corresponding antigen, the green fluorescence protein (GFP). Figure 3 reports representative confocal microscopy images of micro- and nanoscale patterns of antibodies upon biorecognition with the target GFP protein. Stripes patterns of GFPs appeared

quite uniform, even in the submicron range, and protein interactions were observed to be highly specific in the bioactive regions. In fact, although many molecules (especially proteins and antibodies) generally tend to adsorb onto solid surfaces, mainly by hydrophobic interactions [12], the nonfunctionalized areas of our patterned substrates did not show any protein adsorption, as evidenced by the absence of fluorescence background. Moreover, as revealed by the spectral analysis of the solid-state pattern (Fig. 3, right-top), the immobilized GFPs did not show significant conformational changes in the protein core even in the nanoscale features, thus confirming the overall “softness” of the proposed method and the general applicability to reliably pattern functional biomolecules. The accurate micro- and nanopositioning of GFP molecules was also assessed by AFM analyses (Fig. 3, right-bottom), showing well-confined features and a height profile ( $\sim 8$  nm) consistent with the size of the antigen–antibody complex immobilized in air, at ambient conditions.

Finally, as a proof of concept, we demonstrated the possibility to realize parallel patterns of different species, mixed in solution, with accurate spatial control. In this

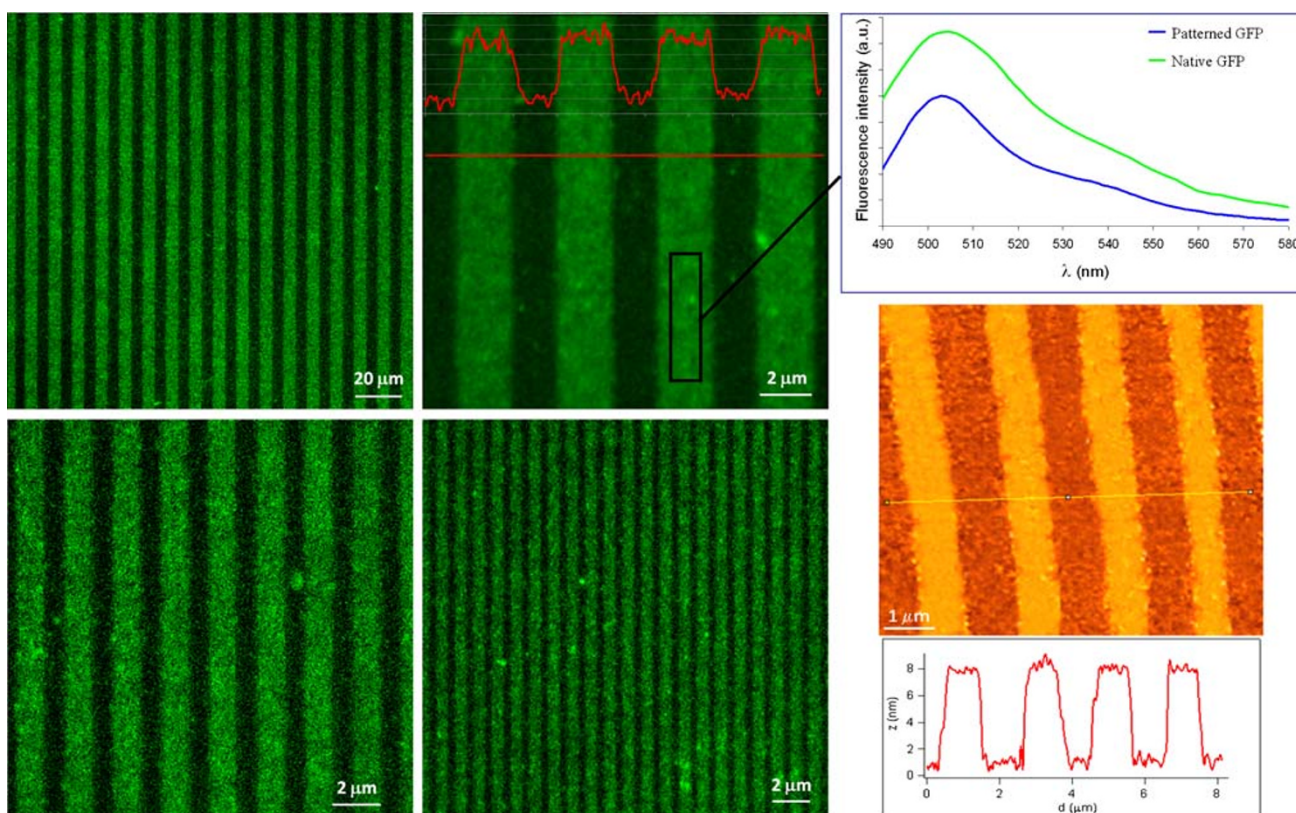


**Fig. 3** Micro- and nanoscale patterning of functional proteins. (Left) confocal microscopy images of stripes of GFPs, with features ranging from 5  $\mu\text{m}$  to 500 nm (a fluorescence line profile is also reported in the inset of the 2  $\mu\text{m}$  wide GFP stripes). (Right, top) Emission

spectrum of patterned GFPs as compared to the native proteins in solution. (Right, bottom) AFM image and line profile of a GFP pattern with 1  $\mu\text{m}$  features

latter case, we wanted to demonstrate the wide versatility of the method, which is therefore not limited to biomolecules, by the site-selective immobilization of two different fluorophores, with potential applications in photonics and material science. To this purpose, we exploited a sequential patterning of thiol- and amine-SAMs in order to produce a smart active substrate that exhibits adjacent regions with different chemical reactivity. We chose two organic/inorganic fluorophores, i.e., fluorescein-5-maleimide (FM) and water-soluble colloidal nanocrystals (NCs), with different chemical reactivities and emitting in two different spectral regions (green and red, respectively), upon single wavelength excitation, thanks to the peculiar broad absorption spectrum of NCs. The overall patterning procedure is illustrated in Fig. 4. After MPTS selective self-assembling onto the EBL-patterned substrate (steps a and b), sequential APTES and glutaraldehyde (GTA) specific immobilization onto the remaining bare SiO<sub>2</sub> regions takes place (step c). The resulting substrate presents alternating patterns of exposed mercapto- and formyl-chemical groups available for the subsequent molecular interactions with an aqueous

mixture of amino-modified NCs (that are going to interact with the activated amino groups) and FM molecules (that are going to interact with the thiol moieties) (step d). Figure 4 (bottom) shows representative confocal microscopy images of the parallel patterning of NCs and FM molecules (stripes and squares, features 10 μm). Both images demonstrate that the patterned chemical reactivity of the substrate was very efficient and specific in selectively recognizing the different species in solutions. The designed features were very homogenous and characterized by a clear spatial confinement of the two fluorophores. The spectral analysis of the different regions (FM, green; NCs, red) disclosed the typical emission spectra of the two fluorophores confirming the high specificity of the patterned substrate (two representative movies of the spectral analysis of the patterned surfaces are also available in the Supporting Information).

In this work, we have demonstrated a very versatile and simple method based on the spatially controlled self-assembling of silane molecules onto EBL-nanopatterned substrates for the site-selective nanopositioning of different

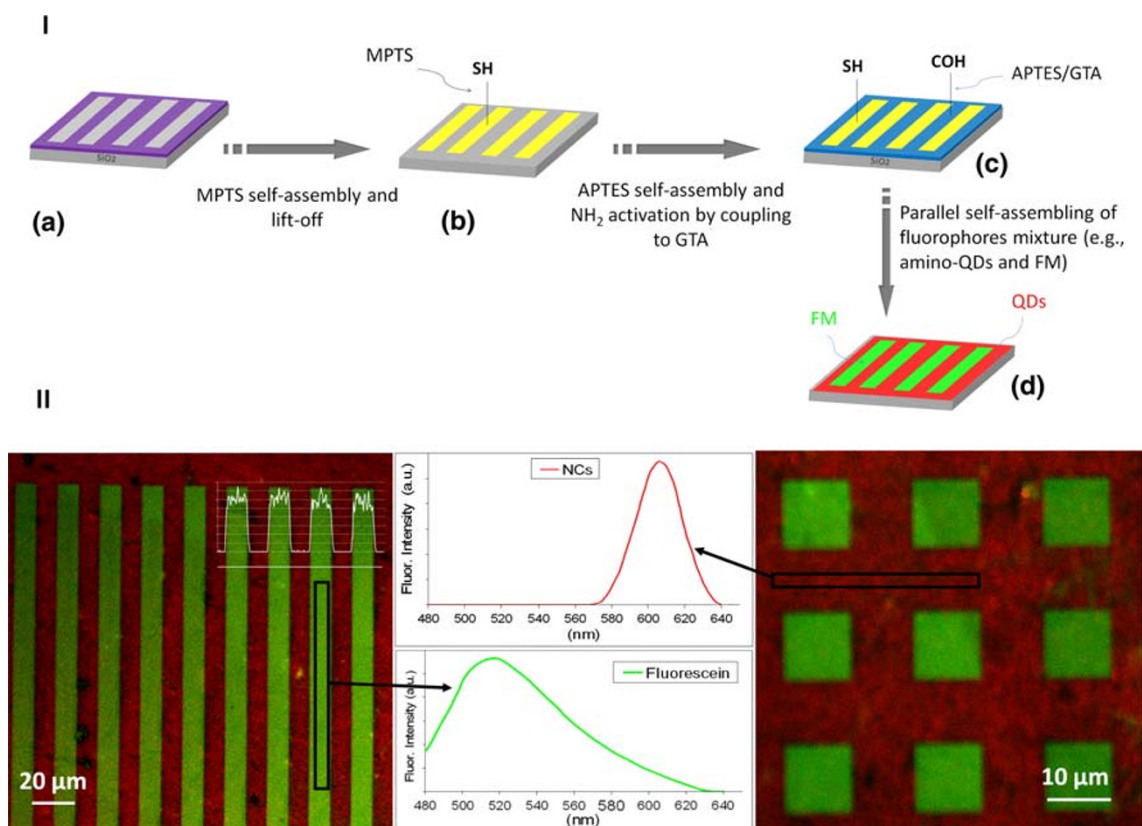


**Fig. 4** **I** Scheme of the process for parallel patterning of a fluorophores mixture (FM and amino-modified NCs). **a, b** MPTS selective self-assembly (SH-SAM) onto a patterned PMMA substrate; **c** sequential patterning of APTES by self-assembly into the exposed SiO<sub>2</sub> regions and subsequent covalent bonding to GTA; **d** parallel site-specific self-assembling of the two fluorophores from an aqueous

mixture onto the patterned substrate. **II** Confocal microscopy images of patterned FM molecules and NCs (stripes and squares, features 10 μm), and spectral analysis of the two patterned regions; a fluorescence line profile of FM molecules (green) is also reported in the inset of the stripes pattern

molecular species. The strategy has a wide applicability as SH- and NH<sub>2</sub>- silanes reactivity is well established and routinely used to link, through specific activating spacers (e.g., GTA, EDC), the most frequent reactive chemical groups of biomolecules and fluorophores (i.e., COOH-, NH<sub>2</sub>-, SH-) [23–26]. The patterned substrates may enable very precise and efficient interactions with a wealth of molecules, including biomolecules, organic fluorophores and water-soluble nanocrystals, leading to the development of hybrid scaffolds of smart bio/inorganic or organic/inorganic active interfaces. Importantly, such hybrid self-assembled structures can be applied in several fields, ranging from diagnostics to optoelectronics. In the case of biomolecules, for instance, such bioactive substrates may open up interesting possibilities to implement novel purification methods onto a solid substrate (e.g., for antibodies or antigens), but also for cell patterning/sorting applications and for single cells studies.

## Experimental

### Micro- and Nanopatterned SAMs: Fabrication and Characterization

Silicon dioxide substrates were treated with a NH<sub>4</sub>OH/H<sub>2</sub>O<sub>2</sub>/H<sub>2</sub>O (1:1:5) solution at 70 °C for 10 min, rinsed with distilled water for 5 min, immersed in HCl/H<sub>2</sub>O<sub>2</sub>/H<sub>2</sub>O (1:1:5) solution at 70 °C for 10 min, rinsed again with distilled water for 5 min, and finally dried with a nitrogen stream. PMMA was then deposited onto the SiO<sub>2</sub> substrates by spin coating, and subsequently baked at 180 °C for 2 min onto an hotplate. EBL was performed by a Leica Lion LV1 system. The exposed PMMA was then developed in a methyl isobutylketone/isopropyl alcohol solution at room temperature. The samples were subsequently dried under a nitrogen stream and treated with oxygen plasma (5 s, 70 mTorr, 25 Watt) in order to remove the PMMA debris and to promote the activation of the SiO<sub>2</sub>-exposed areas, thus improving the surface reactivity for the following SAM deposition. PMMA nanostructures were analyzed by Holographic Microscopy (Lyncée Tec DHM 1000, transmission mode). Afterward, samples were treated for 5 min with a freshly prepared aqueous solution of APTES (0.5% v/v) (Sigma–Aldrich) in order to deposit a cationic layer yielding surface-exposed primary amino groups. Samples were then washed with deionized water for 10 min, dried with a nitrogen stream and stored in a vacuum desiccator overnight, to evaporate physisorbed APTES molecules. The surface density of active chemical groups on the substrate was assessed and quantified by fluorescence measurements, exploiting fluorescein-5-isothiocyanate (FITC, BioChemika, 10 mg/mL stock solution

in DMSO) covalent binding to primary amino groups, and comparison with FITC calibration curve (data not shown). Standard solutions of APTES, ranging from 0.005 to 10% (v/v), were spotted onto the silicon substrates and then incubated with FITC (0.1 mg/mL, over night incubation at 4 °C in the dark). We found that the highest fluorescence signal was obtained with the 0.5% (v/v) value, approximately corresponding to a surface density of exposed amino groups of 22 pmol/cm<sup>2</sup>. The remaining PMMA onto the silanized samples were then removed by soaking samples in hot acetone (10 min), isopropyl alcohol (10 min) and dried with nitrogen flow.

### Glutaraldehyde Cross-Linking

The aminosilanized substrates were activated with a homo-bifunctional linker (glutaraldehyde), suitable to react with aminated probes, such as 5'-aminated ssDNA, antibodies, etc. We used solutions of 2.5% (v/v) glutaraldehyde in 100 mM phosphate buffer, pH 7. The reactions were carried out at 4 °C in the dark for 2 h. Afterward, substrates were abundantly washed with MilliQ water (2 washing cycles for 10 min at ambient temperature), dried with N<sub>2</sub> flow and desiccated in an oven for 3 min at 60 °C.

### Hybridization onto Micro- and Nanopatterned DNA Arrays

Solutions of 0.03 μM ssDNA probes (5'-NH<sub>2</sub>-CGC AGG ATG GCA TGG GGG AG-3') in 1× TE buffer, pH 8.0 were spotted on the micro- and nanopatterned surfaces. After incubating the sample for 2 h in humidified wells at 37 °C, DNA-modified substrates were washed for 3 min with 1× TE solutions and left to dry in air. Also in this case, the surface density of ssDNA was optimized and quantified by fluorescence measurements, using Cy3-labeled ssDNA (5'-NH<sub>2</sub>-CGC AGG ATG GCA TGG GGG AG-Cy3-3') and relative calibration curve (data not shown). We investigated the concentration range of probe DNA from 10 to 0.001 μM, finding an optimal value of 0.03 μM, approximately corresponding to ~0.9 picomol/cm<sup>2</sup> of probe DNA immobilized onto the silicon substrate. Prior to hybridization experiments, activated samples were blocked with NaBH<sub>4</sub>. Hybridization experiments were carried out by investigating the hybridization efficiency of target DNA complementary to the probe (5'-CTC CCC CAT GCC ATC CTG CG-3'), as compared to single-mismatch sequences (5'-CTC CCC CAT ACC ATC CTG CG-3'). In both cases, we used a 10 μM concentration of target DNA in 1× PCR buffer. Finally, in order to detect the fluorescence signal after the hybridization events, we used a solution of 0.5× SYBR Green I in 1× PCR buffer, a typical intercalating dye highly specific for double strand

DNA (1 h incubation at room temperature). After the reaction, samples were washed twice for 10 min with water and gently dried with a stream of nitrogen. High resolution fluorescence imaging was carried out by confocal microscopy (Leica TCS-SP5 AOBS). AFM imaging was performed in air at ambient conditions (20–25 °C, atmospheric pressure, ~50% of humidity) by using a CP-II scanning probe microscope or a Nanoscope IV MultiMode SPM (Veeco, Santa-Barbara, CA), equipped with 5 µm scanners.

### Protein Micro- and Nanoarrays

Functional micro- and nanoarrays of antibodies and proteins were produced by a similar procedure, spotting aqueous solutions of 1 µg/mL of antibodies (Anti-TurboGFP, Evrogen) in 100 mM phosphate buffer onto the glutaraldehyde-activated micro- and nanopatterns (prepared as described above). Reactions were carried out for 4 h in the dark. After antibodies' incubation, the generated Schiff bases were stabilized, and secondary amines linkage with terminal formyl groups were produced by soaking the samples in NaBH<sub>4</sub> for 1 h at room temperature. Afterward, samples were washed in the same buffer with the addition of 0.02% of Tween20 (or 2 mg/mL BSA) in order to prevent the formation of aspecific binding sites. The surface density of antibody molecules was optimized by investigating a wide concentration range of antibodies solutions (from 30 to 0.1 µg/mL), finding an optimal value of 1 µg/mL. Such experiments were performed by exploiting the corresponding fluorescent antigen, i.e., GFP protein. The patterned substrates were always washed by means of a gentle agitation in phosphate buffer for 10 min, and then left to interact with solutions containing GFP proteins (10 µg/mL, rTurboGFP, Evrogen, 1 h in the dark). After gently washing with buffer (10 min, 2 cycles), samples were immediately characterized by confocal microscopy and AFM.

### Parallel Patterning of Organic Fluorophores and Water-Soluble NCs

For these experiments, PMMA micro- and nanostructured substrates were subjected to two sequential different silanes deposition. Initially, samples were incubated with solutions of 0.5% MPTS (v/v) in isopropyl alcohol solution for 1 h at room temperature and then washed three times for 5 min with absolute EtOH, contemporaneously sonicating in order to remove silane aggregates. PMMA was then removed by liftoff and samples were dried under nitrogen stream. Samples were subsequently subjected to the multistep covalent immobilization of 0.5% APTES and

2.5% GTA, following the procedures described above, producing alternating regions with different exposed chemical reactive groups. An aqueous mixture containing the two different fluorophores (0.01% of fluorescein-5-maleimide,  $\lambda_{ex/em}$  492/530 nm, 0.5% stock solution in DMSO, and 0.06 µM of amino-terminated water-soluble nanocrystals, Evident Technologies,  $\lambda_{em}$  610 nm) was spotted onto the active substrates for 4 h in the dark at room temperature. These samples were then washed thoroughly with water, dried with a nitrogen stream and immediately analyzed by confocal microscopy for imaging and spectral analysis.

**Acknowledgments** The authors gratefully acknowledge Barbara Sorce and Loretta L. del Mercato for their help during experiments, and E. D'Amone and V. Fiorelli for the expert technical assistance. This work was supported by the Italian Ministry of Research through MIUR "FIRB" project (RBLA03ER38\_001).

### References

1. M. Stewart, M. Motala, J. Yao, L. Thompson, R. Nuzzo, Proc. Inst. Mech. Engin. Part N J. Nanoengin. Nanosys. **220**, 81 (2006)
2. D.C. Chow, M.S. Johannes, W.-K. Lee, R.L. Clark, S. Zauscher, A. Chilkoti, Mater. Today **8**, 30 (2005)
3. A.E.G. Cass, Electron. Lett. **43**, 903 (2007)
4. J. Ichinose, M. Morimatsu, T. Yanagida, Y. Sako, Biomaterials **27**, 3343 (2006)
5. S. Sabella, G. Vecchio, R. Cingolani, R. Rinaldi, P.P. Pompa, Langmuir **24**, 13266 (2008)
6. F.R.R. Teles, L.P. Fonseca, Mater. Sci. Engin. C **28**, 1530 (2008)
7. A.L. Beaudet, J.W. Belmont, Ann. Rev. Med. **59**, 113 (2008)
8. M. Vasudev, T. Yamanaka, Y. Jianyong, D. Ramadurai, M.A. Stroschio, T. Globus, T. Khromova, M. Dutta, IEEE Sens. J. **8**, 743 (2008)
9. E. Delamar, A. Bernard, H. Schmid, B. Michel, H. Biebuyck, Science **276**, 779 (1997)
10. F. Bretagnol, L. Ceriotti, A. Valsesia, T. Sasaki, G. Ceccone, D. Gilliland, P. Colpo, F. Rossi, Nanotechnology **18**, 135303 (2007)
11. G.-J. Zhang, T. Tanii, T. Funatsu, I. Ohdomari, Chem. Comm. **7**, 786 (2004)
12. G.-J. Zhang, T. Tanii, T. Zako, T. Hosaka, T. Miyake, Y. Kanari, T. Funatsu, I. Ohdomari, Small **1**, 833 (2005)
13. G.-J. Zhang, T. Tanii, Y. Kanari, I. Ohdomari, J. Nanosci. Nanotech. **7**, 410 (2007)
14. S.A. Lange, V. Benes, D.P. Kern, J.K.H. Horber, A. Bernard, Anal. Chem. **76**, 1641 (2004)
15. D.J. Graber, T.J. Zieziulewicz, D.A. Lawrence, W. Shain, J.N. Turner, Langmuir **19**, 5431 (2003)
16. K.-B. Lee, S.-J. Park, C.A. Mirkin, J.C. Smith, M. Mrksich, Science **295**, 1702 (2002)
17. L.M. Demers, D.S. Ginger, S.-J. Park, Z. Li, S.-W. Chung, C.A. Mirkin, Science **296**, 1836 (2002)
18. S.W. Lee, B.-K. Oh, R.G. Sanedrin, K. Salaita, T. Fujigaya, C.A. Mirkin, Adv. Mater. **18**, 1133 (2006)
19. T. Schüller, T. Asmus, W. Fritzsche, R. Möller, Biosens. Bioelectron. **24**, 2077 (2009)
20. G. Gotesman, R. Naaman, Langmuir **24**, 5981 (2008)
21. J.M. Slocik, E.R. Beckel, H. Jiang, J.O. Enlow, J.S. Zabinski Jr., T.J. Bunning, R.R. Naik, Adv. Mater. **18**, 2095 (2006)

22. A. Biasco, D. Pisignano, B. Krebs, P.P. Pompa, L. Persano, R. Cingolani, R. Rinaldi, *Langmuir* **21**, 5154 (2005)
23. G.T. Hermanson, *Bioconjugate techniques* (Academic Press, San Diego, 1996)
24. D.K. Schwartz, *Ann. Rev. Phys. Chem.* **52**, 107 (2001)
25. S. Onclin, B.J. Ravoo, D.N. Reinhoudt, *Angew. Chem. Int. Ed.* **44**, 6282 (2005)
26. C.M. Halliwell, A.E.G. Cass, *Anal. Chem.* **73**, 2476 (2001)